Antenna and Receiver System With Digital Beamforming for Satellite Navigation and Communications

Achim Dreher, *Senior Member, IEEE*, Norbert Niklasch, *Member, IEEE*, Frank Klefenz, and Arno Schroth, *Senior Member, IEEE*

***Abstract*—To demonstrate and investigate the possibilities of active antennas with digital beamforming, a compact breadboard model operating in C-band with planar patches as radiators is fabricated and measured. It was originally designed as a technology demonstrator for navigation purposes, but will be extended for future use in combined navigation and communication systems. Several parameters for beam position, sidelobe reduction, and nulling are set and controlled by a suitable user interface. A special calibration and error-correction procedure is developed to compensate for drift of active elements, mutual coupling of the patches, and finite-ground plane effects. The excellent results demonstrate the versatile features of digital beamforming for satellite navigation and communication systems.**

***Index Terms*—Adaptive antenna, communication system, digital beamforming, navigation system, planar antenna, receiver technology, smart antenna.**

I. Introduction

THE efficiency of future satellite communications and navigation systems can be improved significantly by using adaptive antennas with intelligent beamforming and beam-steering. Interference by multipath propagation or jammers can decisively be reduced by limited beamwidth, sidelobe reduction, and generation of nulls in the direction of the jammer. This leads to a better quality of service (QoS) in communication systems and helps to enhance the accuracy of positioning in navigation systems, which, for instance, is a very important aspect in safety-of-life services.

If communication and navigation systems operate with nongeostationary satellites [low earth orbit (LEO), medium earth orbit (MEO), high elliptical earth orbit (HEO)], only a temporally limited visual contact to a chosen satellite is possible, where the time of contact for LEO satellites can even be below 15 min. The beam of the terminal antenna must follow the course of the satellite and also compensate any movements of a mobile terminal. The latter must take place in any case, i.e., also with geostationary satellites. To determine the terminal position by means of triangulation, the user must have contact to at least four satellites. However, the accuracy of positioning can be improved and the reliability of navigation data increases if more satellites are included. For this purpose, a single steered beam is not sufficient. At least four, better are up to 12 beams, must at the same time automatically track the satellites. Additional beams should comprise a search function for the allocation of rising satellites and a replacement for faulty channels. One beam should serve as replacement. Moreover, interferences must be detected and suppressed by suitable measures in the beamforming process.

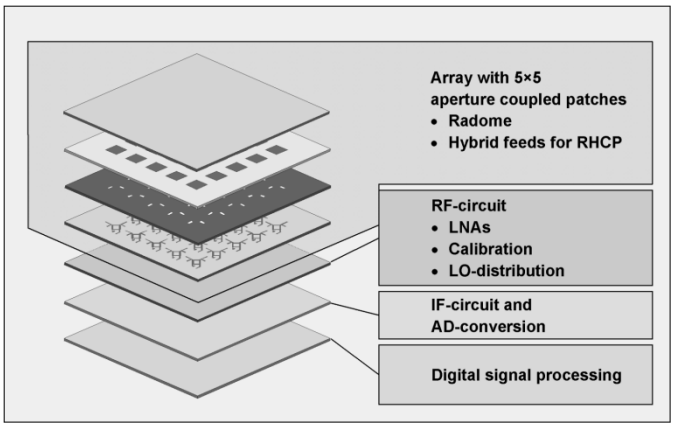

Fig. 1. Arrangement of the terminal antenna modules.

A future-directed technology for the realization of a smart multibeam antenna is digital beamforming [1]. In contrast to conventional phased-array configurations, which require complicated multibeam architectures, no adjustable electronic components are necessary in the RF part. By shifting the beamforming procedure into the digital signal processing (DSP) unit, an enormous increase of flexibility is obtained. The accuracy can still be improved significantly by calibration and suitable error-correction algorithms, to keep the system independent of external physical influences to the largest possible extent.

In combination with planar patches, active elements can be integrated to build complete transmitting and receiving modules. By their flat or also conformal design, they can be integrated particularly well into the surface of vehicles or airplanes.

With increasing progress in digital-processing technology, one of the first experimental setups including a 2×4 array of patch elements operating in S-band was presented in [2]. A linear array of 32 dipoles used as a C-band testbed for algorithm development and demonstration of digital beamforming technology was described in [3]. Rose *et al.* presented an 8×8 two-dimensional array also used as a feed for a larger microwave

Manuscript received September 5, 2002; revised January 29, 2003. This work was supported by the Federal Ministry of Education and Research (BMBF/DLR) under Research Contract 03NB9606/1, Research Contract 50NB9705/5, and Research Contract 50NB9605/7.

A. Dreher, F. Klefenz, and A. Schroth are with the German Aerospace Center, Institute of Communications and Navigation, Oberpfaffenhofen, D-82234 Wessling, Germany.

N. Niklasch is with ViCon Engineering GmbH, D-81249 Munich, Germany.

Digital Object Identifier 10.1109/TMTT.2003.814309

TABLE I
ANTENNA REQUIREMENTS

Hardware	Software
Active antenna array with integrated planar patches	Beamforming capability for up to 12 beams
Frequency range 5.01 – 5.03 GHz	Side-lobe level adjustment
Polarization RHCP	Nulling for jammer suppression
Steering capability Azimuth 360° Elevation ±60°	Adaptive selection and tracking of up to 12 satellites
Gain more than 10 dBi for elevation angles > 15° with the beam pointing at 60° from boresight	Autonomous multipath interference source identification and rejection
System bandwidth 18 MHz	Graphical user interface

lens for pattern experiments [4]. Several other setups for experiments on beamforming and jammer suppression exist [5], [6].

The design, construction, and basic characteristics of an electronically steered antenna for land mobile satellite communications in the L-band are described in [7]. It uses six stacked patches arranged in a circle and includes a global positioning system (GPS) receiver. A phased-array antenna for mobile satellite communications in the L-band for possible use with the Australian Mobilesat system [15] includes broad-band stacked patches in a multilayer design. The conventional beam steering using phase shifters permits transmission and receiving, however, this architecture is not suitable for independent multibeam generation and steering. A pure digital beam-steering antenna for a GPS is presented in [8]. The modular array of up to 16 elements enables up to eight GPS satellites to be tracked. Miura *et al.* report on an experimental digital-beamforming antenna system for mobile communications [9]. Smart antennas with digital beamforming may also play an important role in channel sounding [10].

The digital-beamforming system that we present in this paper is used for experiments, as well as a technology demonstrator for advanced satellite-navigation receivers. It consists of a planar array with 5×5 patches including local-oscillator and calibration-signal distribution. The C-band (5.15 GHz) was used because it is still an option for the future European Galileo satellite system. It needs higher gain antennas in any case and, thus, may take advantage of smart beamforming and interference suppression procedures. The arrays are smaller than in the L-band, which significantly extends the range of application to a larger class of vehicles.

The work performed is the further development of the linear array presented in [11] to a complete planar configuration with integrated RF and signal-processing stages. It was our goal to arrange all components on boards of the same size than the area of the patch layer. The compact breadboard model is measured in a test range. A suitable interface is developed to set different parameters and visualize the actual beamforming features.

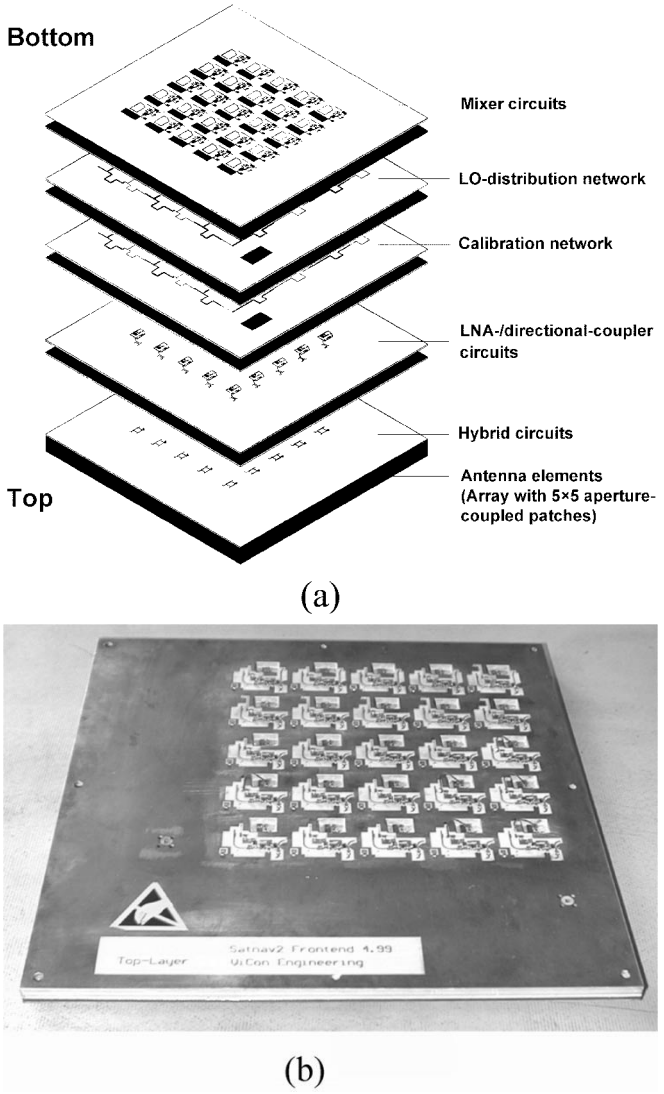

Fig. 2. Layout of RF circuits in multilayer technology. (a) Architecture. (b) Assembled RF multilayer (bottom view).

II. SYSTEM DESCRIPTION

A. Planar Array

In view of future mass production, a compact multilayer structure is designed for the RF structure (Fig. 1). The radiating elements are square patches on the bottom of a thin radome substrate. Each is fed via perpendicular coupling apertures in a ground plane to separate the radiation and feed region. Hybrid couplers are integrated to achieve right-hand circular polarization (RHCP) with sufficient axial-ratio bandwidth and reliable performance. Couplers and feed lines are built

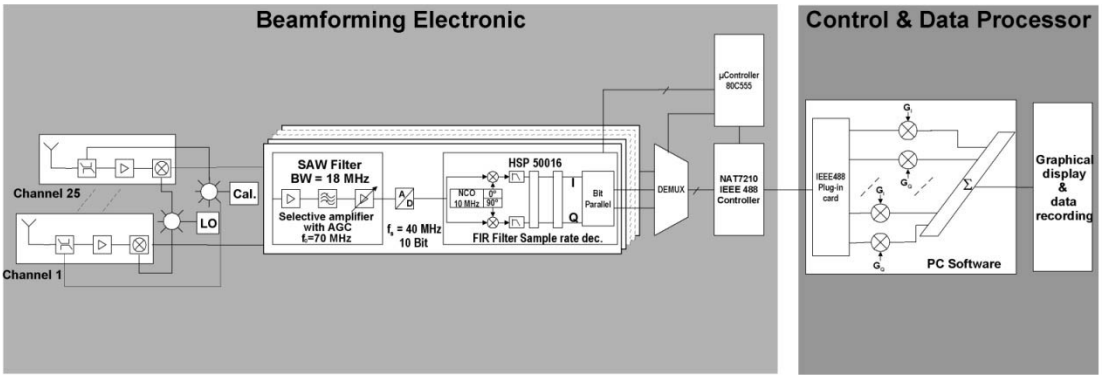

Fig. 3. Block diagram of receiver structure.

in symmetric stripline technology to shield the following electronic components by an additional metallization at the back plane of the antenna. An optimum configuration to meet the requirements listed in Table I is an array of 5×5 radiators with a distance of $\lambda_0/2$, which is mainly a tradeoff between gain, grating lobes, and element coupling. A gain of at least 10 dBi is achieved for elevation angles of 15° if the main beam is scanned to $\pm 60°$ from boresight.

A special problem in stripline structures arising above all in connection with coupling apertures is the generation of parallel-plate modes guided between the metal plates on either side. This may lead to a reduction in efficiency and gain for the single element. The unwanted coupling between the radiators causes a certain degradation of the radiation performance. A special suppression technique to reduce parallel-plate modes without any use of shorting pins [12] was applied and extended to circular polarization [13]. It is based upon shifting the parallel resonant frequency caused by the coupling between the patch and slot to a region, where the loss rate into the parallel-plate mode has its minimum and the patch itself has its resonant frequency. This is achieved by using an additional open-ended stub connected in shunt with the feed line.

Fig. 2(a) shows the bottom view of different layers of the RF part before assembling. The connection of hybrid outputs to the amplifiers [low-noise amplifier (LNA)] is carried out by short vias through the ground plane. To keep losses low, all vias are shielded with shorting pins and the LNAs are mounted directly underneath the hybrids. Additional layers with networks in symmetric stripline technology are used to distribute the signal of the local oscillator to the mixers and to feed a special calibration signal to the input of each LNA. This enables a correction of drift and temperature effects coming from the active elements during the operation of the antenna. The fabricated multilayer structure is depicted in Fig. 2(b).

B. Signal Processing

The receiver structure is shown in Fig. 3. It is based on a heterodyne concept with high digital IF. An input-stage low-noise amplifier monolithic microwave integrated circuit (MMIC) followed by a mixer MMIC forms the analog part used to convert the signal from 5.15 GHz to the first IF of 70 MHz. The complete module has a gain of 18 dB and a single-sideband noise figure of 4.5 dB. To prevent unwanted aliasing effects, the IF

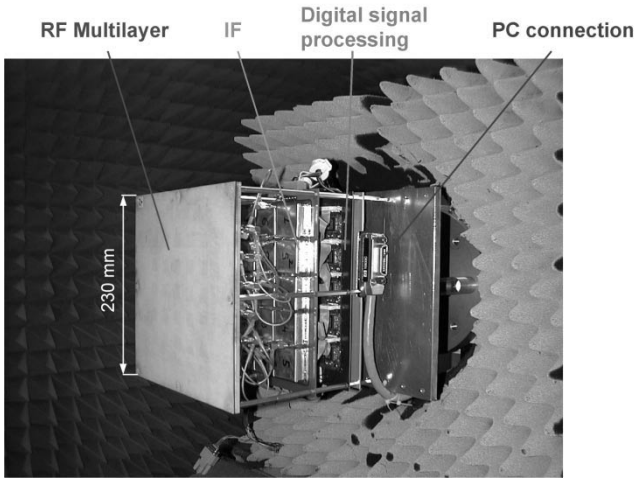

Fig. 4. Complete antenna setup during measurement.

module contains a surface acoustic wave (SAW) filter, which limits the bandwidth to 18 MHz and has a stopband attenuation of at least 50 dB. The level of the IF signal at the AD-converter input is adjusted by means of an amplifier with automatic gain control (AGC). The complete gain of the IF stage is 80 dB. The digital part of the receiver starts with AD conversion that is performed with 10-bit resolution and a sampling rate of 40 MS/s.

Basically, satellite-navigation signals are processed using 1–3-bit quantization only due to the signal being buried in noise and the low dynamics in the amplitudes of the signal. When applying beamforming, the dynamics in signal amplitude, i.e., the signal level of the main lobe compared to the sidelobes or the deep nulls being generated, will be increased significantly. This results in a demand for a higher resolution in quantization. The actual 10-bit resolution has been selected based on an analysis of the influence on the settings of the amplitude and phase weights, as well as the resulting influence on the calculated radiation patterns. Resolutions of ten bits and more result in dynamic ranges of over 60 dB, phase errors less than 0.5°, and signal quantization to noise power ratio degradation due to sampling better than 60 dB, which is well within the specification requirements. In addition, the availability of commercial low-power and cost-efficient integrated circuits (ICs) has been taken into account.

The presented concept generates a second IF at 10 MHz by utilizing undersampling. After that, the digitized signal is trans-

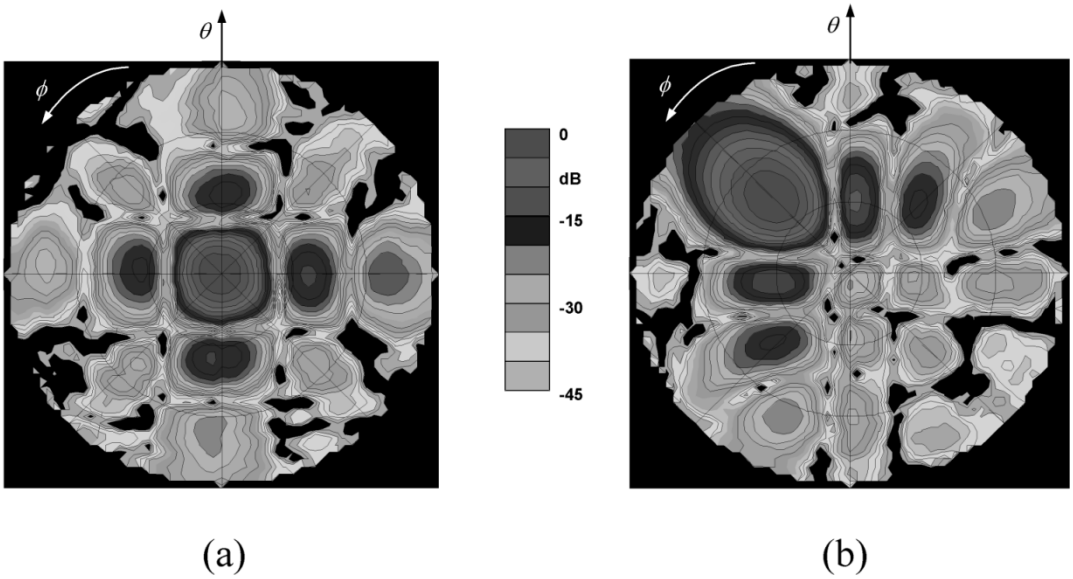

Fig. 5. Measured radiation characteristics of digital antenna for different scan angles at center frequency (5.15 GHz). (a) $\varphi = 0°, \theta = 0°$. (b) $\varphi = 45°, \theta = 45°$.

formed to baseband and decomposed to in-phase and quadrature components. This is done in a special IC (HSP50016). The highest output rate of the digital converter is adjusted to 1 kHz, but with the tuning ability of the converter, a frequency sweep over the whole bandwidth of 16 MHz is possible. The channels of the beamforming electronic show a crosstalk of less than -25 dB.

An intelligent interface consisting of a microprocessor and an IEEE 488 controller chip is used to organize the data transfer via the IEEE 488 standard bus. The final beamforming is accomplished via a personal computer (PC).

III. Beamforming Algorithms

Special beamforming methods are used to generate beams to given directions. The level of sidelobes can be adjusted and deep nulls can be generated in the direction of jammers and interferers. Different algorithms for sidelobe-level adjustment and nulling based on binomial, Taylor and Chebyshev approximations derived from linear arrays were implemented. In addition, it is possible to directly apply independently calculated weights and observe the resulting effects. At the moment, no adaptive algorithms are implemented.

To achieve good results, the single-element radiation patterns, strongly depending on the position of the radiator within the array and determined by mutual coupling and finite ground plane, was taken into account and used for the error-correction procedure. The radiation pattern of the embedded element m of a planar array of arbitrary shape with the infinite ground plane is given as

$$E_m^{\mathrm{em}}(\theta,\phi) = E^{\mathrm{is}}(\theta,\phi)\sum_{n=1}^{N} c_{mn} e^{-jk_0(x_n u(\theta,\phi)+y_n v(\theta,\phi))} \quad (1)$$

with $u(\theta,\phi) = \sin(\theta)\cos(\phi)$ and $v(\theta,\phi) = \sin(\theta)\sin(\phi)$. $E^{\mathrm{is}}(\theta,\varphi)$ denotes the ideal isolated pattern of the array elements, c_{mn} are the coupling coefficients, and N is the total number of elements.

Introducing the decoupling matrix $\boldsymbol{DC}_{(N\times N)}$ as the inverse of the coupling matrix $\boldsymbol{C}_{(N\times N)}$, the isolated pattern of the array elements can be evaluated from

$$\begin{bmatrix} E_1^{\mathrm{is}} \\ \vdots \\ E_N^{\mathrm{is}} \end{bmatrix} = \boldsymbol{DC}_{(N\times N)} \begin{bmatrix} E_1^{\mathrm{em}} \\ \vdots \\ E_N^{\mathrm{em}} \end{bmatrix}. \quad (2)$$

It is also used to determine the corrected weighting vector $\boldsymbol{w}^c_{(N)}$ by multiplying the transposed decoupling matrix with the original weighting vector $\boldsymbol{w}_{(N)}$ [14]

$$\begin{bmatrix} w_1^c \\ \vdots \\ w_N^c \end{bmatrix} = \boldsymbol{DC}^T_{(N\times N)} \begin{bmatrix} w_1 \\ \vdots \\ w_N \end{bmatrix}. \quad (3)$$

However, this method still assumes infinite ground planes.

In order to take finite ground-plane effects into account, the ideal isolated patterns in (1) have to be replaced by the real isolated patterns in a finite ground-plane environment

$$E_m^{\mathrm{em}}(\theta,\phi) = \sum_{n=1}^{N} c_{mn} f_n$$
$$f_n = E_n^{isr}(\theta,\phi) e^{-jk_0(x_n u(\theta,\phi)+y_n v(\theta,\phi))} \quad (4)$$

where E^{isr} is the real measured pattern of a single element in a finite ground-plane arrangement.

Equation (4) is solved in a least-squares process using real measured data as input values. In order to achieve adequate precise results for planar arrays, at least 18 evaluation planes in ϕ, θ-cuts, and evaluation steps smaller than 4° per evaluation plane have to be incorporated in the least-squares fit process.

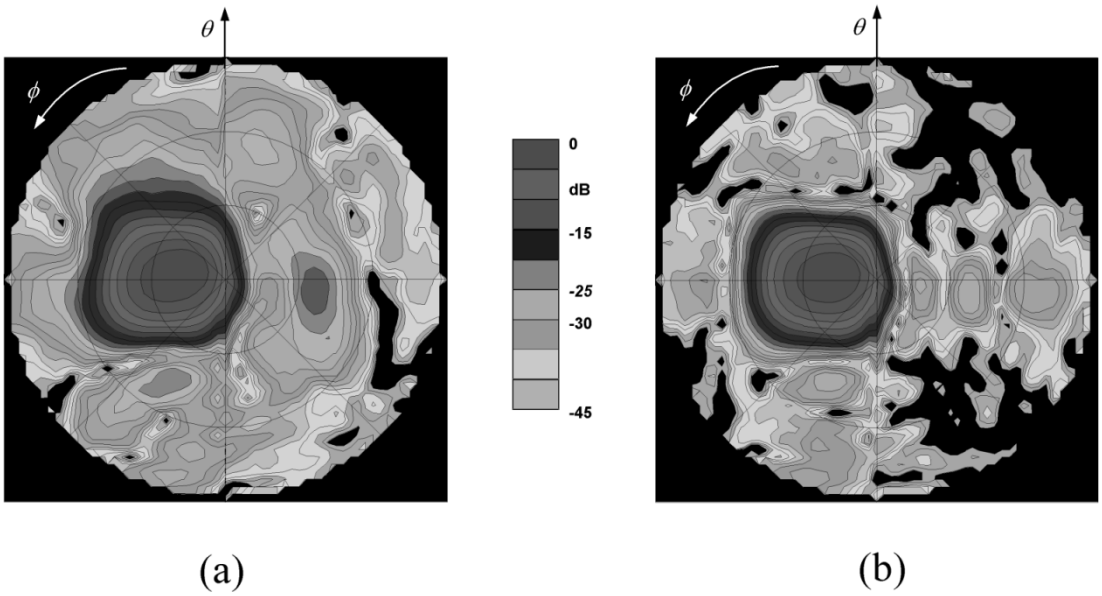

Fig. 6. Scan with $\varphi = 90°$ and $\theta = 20°$ using additional sidelobe control (< -25 dB). (a) Without compensation of mutual coupling and finite ground plane. (b) With compensation.

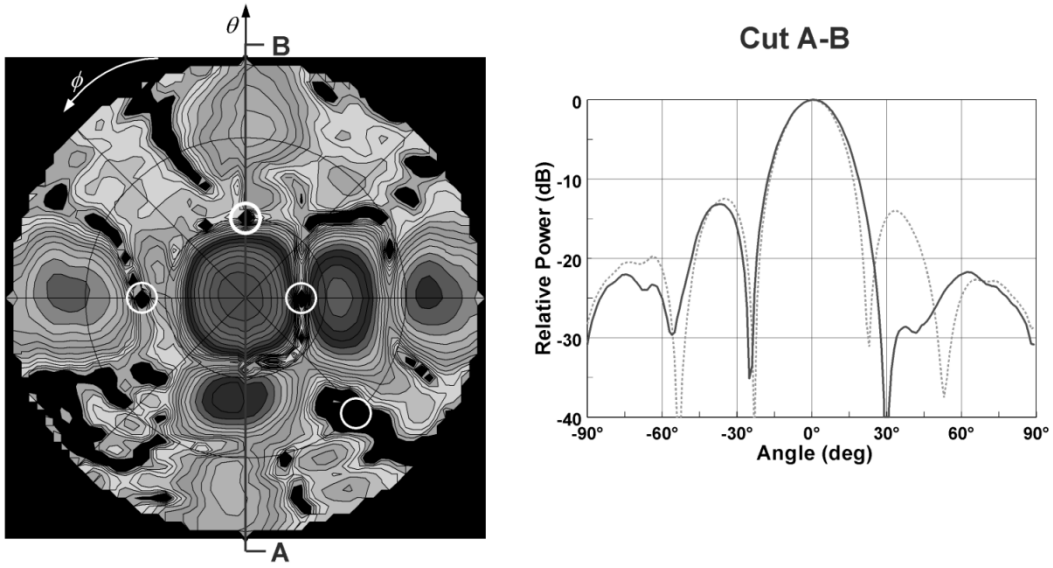

Fig. 7. Multiple pattern-null generation at $(\varphi, \theta) = (0°, 30°)$, (90°, 39°), $(-135°, 60°)$, $(-90°, 21°)$. The cut for $\varphi = 0°$ shows the radiation characteristic with (—) and without (- - -) pattern null at (0°, 30°).

To mitigate a detected interfering signal, the weights have to be calculated in such a way that a null value is placed into the direction of incidence of the interfering signal. The procedure used here is based on Schelkunoff's method [16]. The concept is developed on the fact that rectangular arrays can be treated as a superposition of two orthogonal linear arrays. This allows utilizing algorithms developed for linear arrays. A linear array consisting of N elements allows the placing of $N-1$ zeros. The radiation pattern of the planar array can be calculated through the product form of a polynomial representation of two orthogonal linear arrays

$$AF(\theta,\phi) = \sum_{i=1}^{N}\sum_{k=1}^{M} w_{ik} e^{jk_0 d((i-1)u+(k-1)v)}$$

$$\begin{aligned} &= \left(\sum_{i=1}^{N} w_{Vi}\cdot e^{jk_0 d_z (i-1)u}\right) \\ &\quad\cdot\left(\sum_{k=1}^{M} w_{Hk}\cdot e^{jk_0 d_y (k-1)v}\right) \\ &= \prod_{i=1}^{N-1}\left(e^{jk_0 d_z \sin(\theta)\cos(\phi)} - q_i\right) \\ &\quad\cdot \prod_{k=1}^{M-1}\left(e^{jk_0 d_y \cos(\theta)\sin(\phi)} - q_k\right) \end{aligned} \tag{5}$$

where q_i and q_k are the zeros of the radiation characteristic of the two linear arrays, and d_x and d_y are the geometrical distances between elements in the x- and y-directions, respectively.

The zeros can be placed at any wanted direction. The related weighting coefficients w_{Vi} and w_{Hk} are derived by comparing the coefficients of the two polynomials.

IV. Results

The complete antenna was characterized in a test range (Fig. 4). Several parameters were adjusted using a PC and a suitable interface, which was also used for data recording and graphical representation. All measurements were carried out at center frequency (5.15 GHz). The capability of exact beam positioning was demonstrated for a scan angle of $-180° \leq \phi \leq 180°$ and $0° \leq \theta \leq 60°$. Fig. 5 shows a surface plot with a zenith-directed beam and two-dimensional scanning with $\phi = 45°$ and $\theta = 45°$.

An example for sidelobe suppression with simultaneous scanning is shown in Fig. 6. For all scan angles in the given region, the sidelobe level can be kept lower than -25 dB. The generation of multiple very deep nulls was also demonstrated (Fig. 7). The attenuation of the signal from these directions is more than -45 dB and there is only little influence on the shape of the main beam. Exact positioning and the considerable deepness of the nulls show the efficiency of the error-correction algorithm.

V. Conclusions

A compact breadboard model of a C-band antenna with digital beamforming was designed, manufactured, and tested. It consisted of a planar array with 5×5 patches fed with a 90°-hybrid and slot coupling to achieve circular polarization. The array was build up in a multilayer structure together with a radome and networks to distribute local-oscillator and calibration signals. All components including DSP were arranged underneath the radiators on printed circuit boards of the same size. With this, a first and important successful step was taken to a complete integration of the antenna. The extensive and excellent test results have shown the numerous advantages and flexibility of this kind of antenna.

References

[1] J. Litva and T. K. Lo, *Digital Beamforming in Wireless Communications*. Norwood, MA: Artech House, 1996.

[2] D. C. D. Chang, W. N. Klimczak, and G. C. Busche, "An experimental digital beamforming array," in *IEEE AP-S Int. Symp. Dig.*, Syracuse, NY, June 1988, pp. 1300–1303.

[3] L. J. Simonangeli and A. Agrawal, "A C-band digital beamforming array," in *IEEE AP-S Int. Symp. Dig.*, Syracuse, NY, June 1988, pp. 1385–1388.

[4] J. F. Rose, B. A. Worley, and M. M. Lee, "Antenna patterns for prototype two-dimensional digital beamforming array," in *IEEE AP-S Int. Symp. Dig.*, Ann Arbor, MI, June 1993, pp. 1544–1547.

[5] J. Herd, "Experimental results from a self-calibrating digital beamforming array," in *IEEE AP-S Int. Symp. Dig.*, Dallas, TX, May 1990, pp. 384–387.

[6] R. Baseri, K.-B. Yu, and M. A. Hussain, "Testing adaptive jamming cancellation algorithms using a digital beamforming array," in *Proc. IEEE Nat. Radar Conf.*, Syracuse, NY, May 1997, pp. 314–319.

[7] J. I. Alonso *et al.*, "Low-cost electronically steered antenna and receiver system for mobile satellite communications," *IEEE Trans. Microwave Theory Tech.*, vol. 44, pp. 2438–2448, Dec. 1996.

[8] A. Brown and R. Silva, "A GPS digital phased array antenna and receiver," in *Proc. IEEE Int. Phased Array Systems Technology Conf.*, Dana Point, CA, May 2000, pp. 153–156.

[9] R. Miura, T. Tanaka, I. Chiba, A. Horie, and Y. Karasawa, "Beamforming experiment with a DBF multibeam antenna in a mobile satellite environment," *IEEE Trans. Antennas Propagat.*, vol. 45, pp. 707–714, Apr. 1997.

[10] R. S. Thomä, D. Hampicke, A. Richter, G. Sommerkorn, and U. Trautwein, "MIMO vector channel sounder measurement for smart antenna system evaluation," *Eur. Trans. Telecommun.*, vol. 12, no. 5, pp. 427–438, Sept. 2001.

[11] A. Dreher, T. Hekmat, N. E. Niklasch, M. Lieke, F. Klefenz, and A. Schroth, "Planar digital-beamforming antenna for satellite navigation," in *IEEE MTT-S Int. Microwave Symp. Dig.*, Anaheim, CA, June 1999, pp. 647–650.

[12] M. Yamamoto and K. Itho, "Slot-coupled microstrip antenna with a triplate line feed where parallel-plate mode is suppressed," *Electron. Lett.*, vol. 33, pp. 441–443, Mar. 1997.

[13] A. Dreher, F. Klefenz, and S. Gupta, "Multilayer technology for smart antennas in user terminals," in *Antennas and Propagation Millennium Antennas Propagat. Conf.*, vol. 1, Davos, Switzerland, Apr. 2000, CD ROM.

[14] T. Hekmat, S. Mathiae, and N. Niklasch, "Pattern imbalance effects and their compensation in small microstrip arrays," in *Antennas and Propagation Millennium Antennas Propagat. Conf.*, vol. 1, Davos, Switzerland, Apr. 2000, CD ROM.

[15] M. E. Bialkowski and N. C. Karmakar, "A two ring circular phased-array antenna for mobile satellite communications," *IEEE Antennas Propagat. Mag.*, vol. 41, pp. 14–23, June 1999.

[16] C. A. Balanis, *Antenna Theory: Analysis and Design*. New York: Wiley, 1997.

Achim Dreher (M'92–SM'99) was born in Hermannsburg, Germany, in 1955, He received the Dipl.-Ing. (M.S.) degree from the Technische Universität Braunschweig, Braunschweig, Germany, in 1983, and the Dr.-Ing. (Ph.D.) degree from the FernUniversität, Hagen, Germany, in 1992, both in electrical engineering.

From 1983 to 1985, he was a Development Engineer with Rohde & Schwarz GmbH & Company KG, Munich, Germany. From 1985 to 1992, he was a Research Assistant, and from 1992 to 1997, he was a Senior Research Engineer with the Department of Electrical Engineering, FernUniversität. Since 1997, he has been with the German Aerospace Center (DLR), Oberpfaffenhofen, Germany, as Head of the Antenna Research Group. His current research interests include analytical and numerical techniques for conformal antennas and microwave structures, smart antennas for satellite communications and navigation, and antenna technology for radar applications.

Norbert Niklasch (M'93), photograph and biography not available at time of publication.

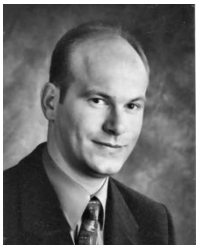

Frank Klefenz received the Dipl.-Phys. (M.S.) degree from the University of Heidelberg, Heidelberg, Germany, in 1997.

From 1996 to 1998, he was with the Max-Planck-Institut für Kernphysik, Heidelberg, Germany, and Deutsches Elektronen-Synchrotron (DESY), Hamburg, Germany, initially working toward the Dipl.-Phys. (M.S.) degree and later as a Research Assistant involved in the field of high-frequency design. Since 1998, he has been a Research Assistant with the German Aerospace Center (DLR), Oberpfaffenhofen, Germany. His current research interests include the application of numerical methods in antenna technology and the design and development of passive and active antennas for communications, navigation, and radar applications.

Arno Schroth (M'89–SM'93) was born in Mallersdorf, Germany, on June 14, 1943. He received the Dipl.-Ing. and Dr.-Ing. degrees in electrical engineering from the Technical University of Munich, Munich, Germany, in 1968 and 1971, respectively.

In 1989 he became an Academic Lecturer and, in 1993, a Professor with the University of the West German Armed Forces, Munich, Germany. In 1969, he joined the German Aerospace Research Establishment (DLR) (formerly DFVLR), Oberpfaffenhofen, Germany, where he was involved in research activities and projects in the field of antennas and propagation, satellite communications, and satellite navigation, as well as radar techniques. From 1983 to 1999, he was Head of the RF Physics Division, Institute for Radio Frequency Technology. He is currently Head of the Navigation and Guidance Systems Division, Institute of Communications and Navigation and Deputy Director of this institute. His current research interests are in satellite communications and navigation, as well as air-traffic control and guidance techniques. He has authored or coauthored over 100 scientific papers in electronics. From 1986 to 1989 he was an Associate Editor of *ntz Archiv*, the scientific journal of the German Society in Information Technology (ITG). He is a member of the Scientific Board of the newly founded *European Transactions on Telecommunications and Related Technologies* (ETT).

Dr. Schroth is a member of the ITG (formerly NTG). He was the recipient of the 1978 DLR Award and the 1985 Premium Award of the International Conference on Antennas and Propagation (ICAP).